

**GLOBAL JOURNAL OF ENGINEERING SCIENCE AND RESEARCHES**  
**Fe<sub>2</sub>O<sub>3</sub>/Cu<sub>2</sub>S CORE-SHELL THIN FILMS: EFFECT OF ANNEALING TEMPERATURE**  
**ON MICROSTRUCTURAL, OPTICAL AND SOLID STATE PROPERTIES**

R.O. Okoro<sup>\*1,3</sup> & M. N. Nnabuchi<sup>1,2</sup>

<sup>\*1</sup>Department of Industrial Physics, Ebonyi State University, Abakaliki, Nigeria

<sup>2</sup>Department of Physics, University of Agriculture, Umudike, Nigeria

<sup>3</sup>Department of Physics, Ebonyi State College of Education, Ikwo, Ebonyi State, Nigeria

**ABSTRACT**

*Fe<sub>2</sub>O<sub>3</sub>/Cu<sub>2</sub>S core-shell thin films were successfully deposited on glass substrates using chemical bath deposition technique. The films were characterized for microstructural and optical properties using scanning electron microscope and spectrophotometer respectively. The scanning electron microscopy studies indicated an increase in particle size and uniformity of particle distribution with annealing temperature. The optical results showed that absorbance (A) increased with annealing temperature in the range of  $0.05 \leq A \leq 0.58$  for as-grown sample,  $0.13 \leq A \leq 0.68$  for annealed at 150°C and  $0.20 \leq A \leq 0.93$  for annealed at 200°C. Transmittance,  $T \leq 92\%$  for as-grown sample,  $T \leq 87\%$  for annealed at 150°C and  $T \leq 63\%$  for annealed at 200°C. Absorption coefficient,  $\alpha$  increased from  $0.1 \times 10^6 \text{ m}^{-1}$  to  $1.45 \times 10^6 \text{ m}^{-1}$  for as-grown sample,  $\alpha$  increased from  $0.12 \times 10^6 \text{ m}^{-1}$  to  $1.63 \times 10^6 \text{ m}^{-1}$  for annealed at 150°C and  $\alpha$  increased from  $0.4 \times 10^6 \text{ m}^{-1}$  to  $2.20 \times 10^6 \text{ m}^{-1}$  for annealed at 200°C. The band-gaps were found to be 3.90eV, 3.80eV and 3.70eV for as-grown, annealed at 150°C and 200°C respectively. The properties of high transmittance in the visible region and wide direct band gap of the films suggest that they can be used as window layers in a heterojunction solar cell as well as in optoelectronic applications.*

**Keywords:** chemical bath deposition, band gap, absorbance, transmittance, microstructure.

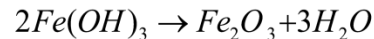
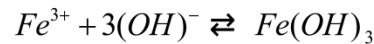
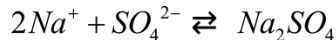
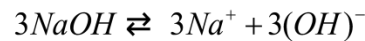
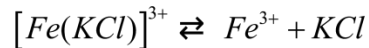
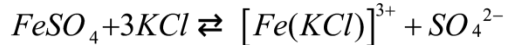
**I. INTRODUCTION**

Energy generation is apt and strategically important to industrialization and meaningful developments in any nation of the world. Non-availability and high cost of energy have remained a huge challenge in many nations including Nigeria which ostensibly had affected many sectors of the economy and indeed, the quest for industrialization. Presently, Nigeria energy mix is dominated by fossil fuels which have been associated with a number of climatic and environmental problems such as acid rain, global warming and ozone layer depletion. Consequently, the world today is searching for new sources of cleaner energy that would not only lead to sustenance of industrialization but also preserve the earth for the future generations. The energy demands have recently spurred greater interests of the solid state scientists, to look inward in the direction of solar energy conversion through semi-conductive materials. The major problem is that, despite the huge solar energy potential in Nigeria, it has not been fully harnessed for commercial purposes due to high cost of solar energy conversion devices. Research has shown that the cost of solar energy conversion devices can be significantly reduced if they are made up of thin film materials. Thin films of II-VI semiconductors exhibit high efficiencies, they have high absorption co-efficient and have direct band gap, the values of which correspond to the wide range of solar spectrum [1]. This makes them promising materials for the photovoltaic device application. Fe<sub>2</sub>O<sub>3</sub> and CuS are important group 11-VI semiconductors materials with myriad of applications. Moreso, the constituent elements are abundant in nature and poses no direct contamination of the environment. Fe<sub>2</sub>O<sub>3</sub> is the most stable oxide of iron and is environmentally friendly (non-toxic), highly resistant to corrosion and ferromagnetic [2]. It occurs naturally in the form of a mineral resource called hematite which is the major source of iron used in producing steel [3]. In the form of fine powder,  $\alpha$ -Fe<sub>2</sub>O<sub>3</sub> is used in polishing metallic jewelry and lenses [4]. Alpha-Fe<sub>2</sub>O<sub>3</sub> is used as catalyst for petrochemical applications [5] and also has biomedical applications [6,7].

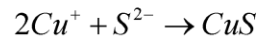
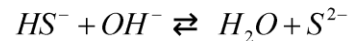
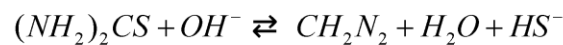
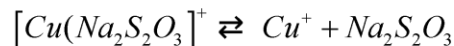
The integration of the two binary thin films into a core-shell of the type  $Fe_2O_3/Cu_2S$ , has the potential of tailoring the band gap for specific applications. In general, the formation of core-shell enhances the properties of materials through synergetic or complementary behaviours between the core and shell materials. The reinforcement or modification of each component can manifest fascinating synergetic properties or multifunctionalities. Various authors have reported on the effect of annealing temperature on chemically deposited core-shell thin films [8-14]. In this present work, we contribute by investigating the effect of annealing temperature on  $Fe_2O_3/Cu_2S$  core-shell thin films grown by chemical bath deposition technique.

## II. EXPERIMENTAL

First,  $Fe_2O_3$  film will be deposited from chemical bath containing 10-20mls, 0.5M-1.5M of  $FeSO_4 \cdot 7H_2O$ , 10-20mls of 0.5M-1.5M of KCl, 2-4 drops of 1M of NaOH (complexing agent) and 38-50mls of distilled water in that order with  $P^H$  between 3.3-3.6 at 60°C bath temperature. for 2 hours. To deposit  $Fe_2O_3/Cu_2S$  ternary thin films, the glass substrates containing  $Fe_2O_3$  deposits will be inserted into a chemical bath containing 3-16mls, 0.1-0.7M of  $CuCl_2$ , 2-6mls of 0.1-0.3M of  $(NH_2)_2CS$ , 4-10mls of  $Na_2S_2O_3$  (complexing agent) and 70-80mls of distilled water at 60°C bath temperature with  $P^H$  in the range 9.7-10 for 90 minutes. The step wise ionic reaction involved in the complex ion formation and film deposition processes for  $Fe_2O_3$  films are as follows [15].



The possible chemical reactions for the formation of  $Cu_2S$  thin film proceeded as follows [16].



The transmittance measurement was done using UNICO-UV-2012 PC spectrophotometer from which other optical and solid state properties of the films were calculated using mathematical relations.

## III. RESULTS AND DISCUSSION

Rutherford backscattering (RBS) was used to determine the elemental composition, depth profile and thicknesses of the film samples by Proton Induced X-ray Emission (PIXE) scans on the samples from a Tandem Accelerator Model 55DH 1.7MV Pellaton. A typical RBS micrograph of the films is shown in Fig.1. The chemical status and elemental composition for as-grown  $Fe_2O_3/Cu_2S$  thin film sample comprises 1.05% iron (Fe), 98.95% oxygen (O), 2.76% copper (Cu) and 11.39% sulphur (S) confirming the formation of  $Fe_2O_3/Cu_2S$  thin film. The glass substrate comprises 34% silicon (Si), 26% oxygen (O), 6% calcium (Ca), 25% sodium (Na), 5.2% aluminium (Al), 3.5% potassium (K) and 0.30% iron (Fe).

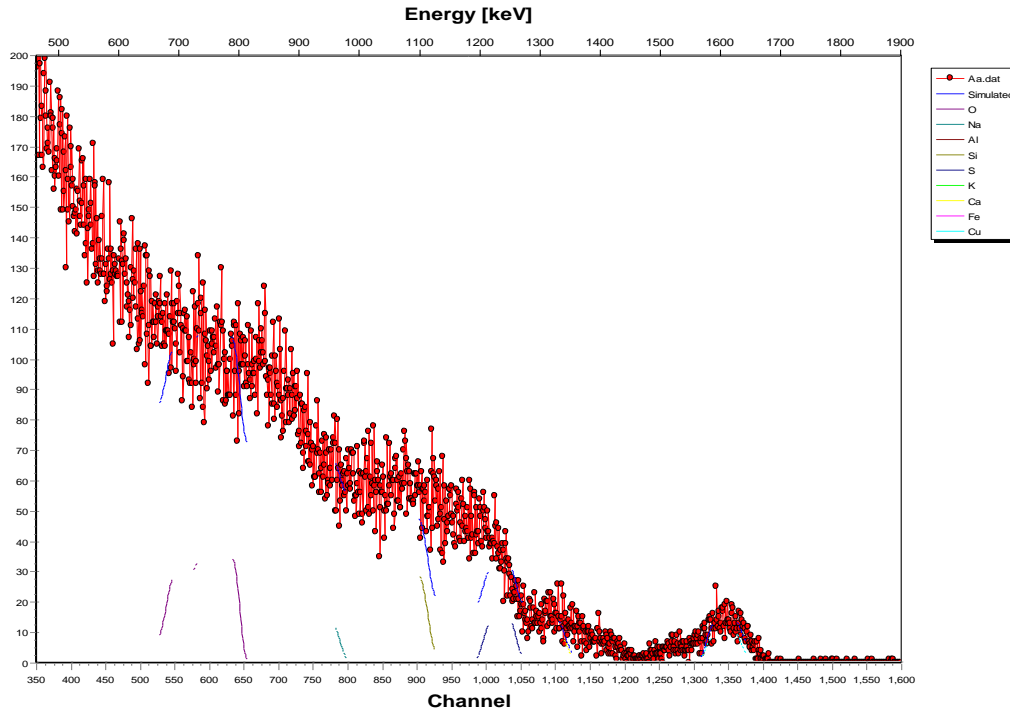


Fig.1: RBS micrograph for as-grown  $Fe_2O_3/Cu_2S$  thin film

Scanning electron microscopes is a versatile technique for studying microstructure of thin film. The microstructure of the films for as-grown, annealed at 150°C and 200°C are shown in figures 2, 3 and 4 respectively. A glance on the microstructures showed an increase in particle size with annealing temperature. It can also be observed that at higher annealing temperature, the uniformity of the crystal tends to increase. Fig. 4 represents a denser structure with homogeneously distributed large grains and well-defined grain boundaries. These findings are in agreement with the report of Augustine and Nnabuchi (2017) for PbS-NiO-CdO thin films [17].

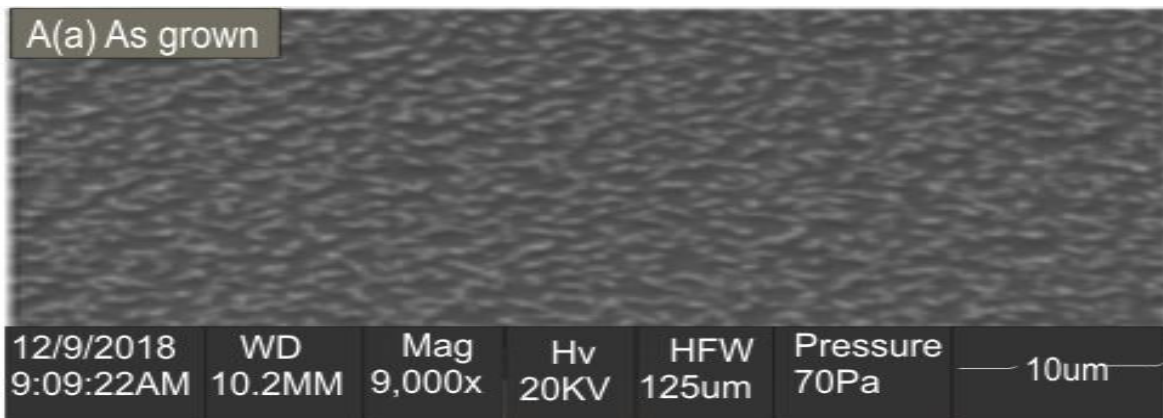


Fig.2: Microstructure for as-grown  $Fe_2O_3/Cu_2S$  thin film

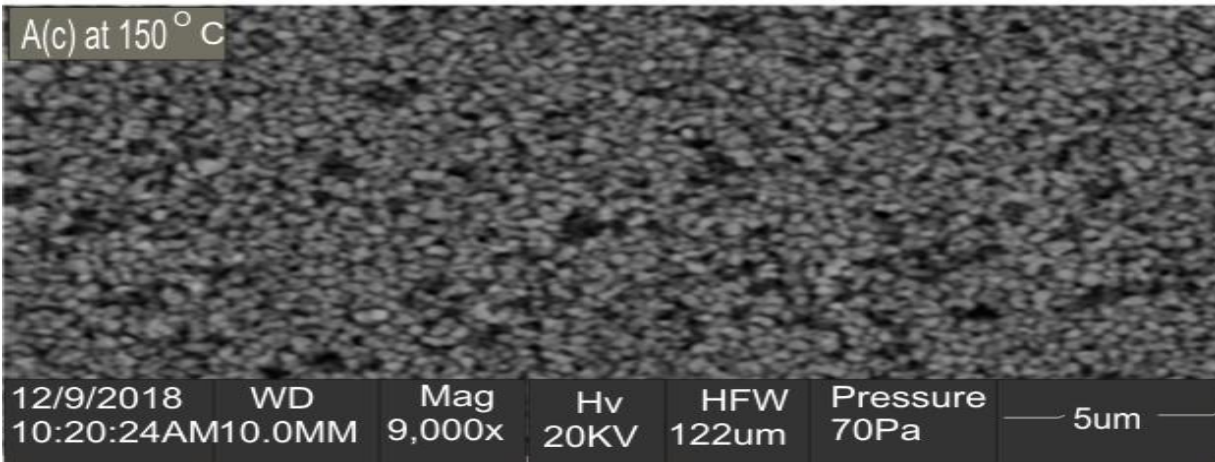


Fig.3: Microstructure for  $Fe_2O_3/Cu_2S$  thin film annealed at  $150^\circ C$

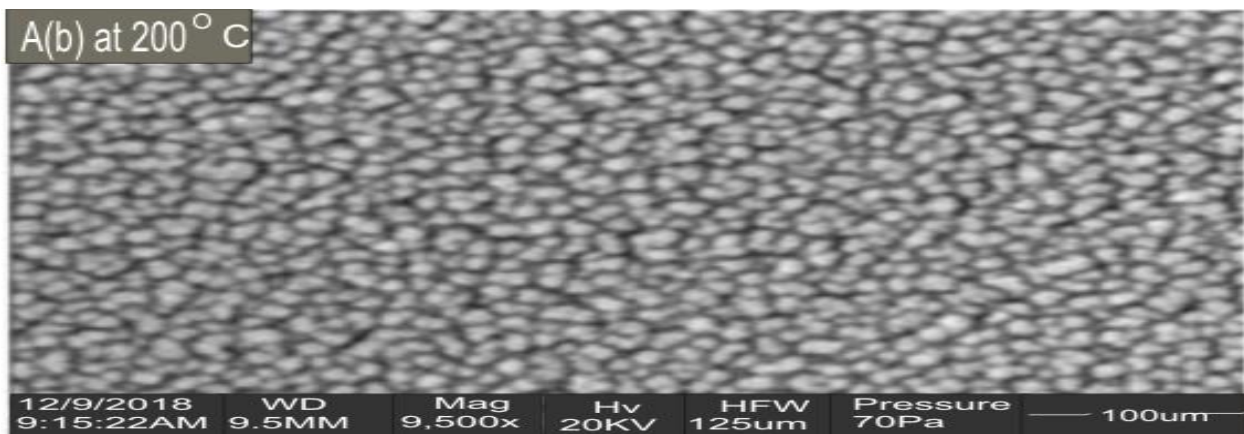


Fig.4: Microstructure for  $Fe_2O_3/Cu_2S$  thin film annealed at  $200^\circ C$

The variations of absorbance with wavelength is shown in Fig. 5. The parametric studies involving the variation of annealing temperature, showed that the optical absorbance increased linearly with annealing temperature exhibiting a maximum for annealed at  $200^\circ C$ . This observation is not unconnected with increase in particle size associated with increase in temperature. In all deposition parameters, absorbance of the films in UV-VIS-NIR is found to decrease with increase in wavelength. The absorbance,  $A$ , generally lie in the range  $0.05 \leq A \leq 0.58$  for as-grown sample,  $0.13 \leq A \leq 0.68$  for annealed at  $150^\circ C$  and  $0.20 \leq A \leq 0.93$  for annealed at  $200^\circ C$ . The absorbance values are within the range stipulated by Lambert-Beer's law [18]. These findings are similar to our precious report on ZnS/ $Fe_2O_3$  core-shell thin films [19]. High absorbance in the UV region as depicted by  $Fe_2O_3/Cu_2S$  thin film makes the material useful in formation of p-n junction solar cells with other suitable materials for photovoltaic applications [20]. The plot of transmittance against wavelength is presented in Fig.6. The spectral transmittance showed that transmittance decreased with annealing temperature exhibiting a minimum for film sample annealed at  $200^\circ C$ . In the UV region, the transparency of the films vary from 25-80%, 20-55% and 12-30% for as-grown, annealed at  $150^\circ C$  and  $200^\circ C$  respectively. In the visible region, the transparency vary from 80-88%, 55-85% and 30-65% for as-grown, annealed at  $150^\circ C$  and  $200^\circ C$  respectively. In the infrared region, the transmittance of the films vary from 90-92% for as-grown, 85-87% for annealed at  $150^\circ C$  and 63-60% for annealed at  $200^\circ C$ . The annealing temperature effect on optical transmittance of thin films have been reported by other research group [8-14, 21-23]. The transmittance characteristics of  $Fe_2O_3/Cu_2S$  core-shell thin films suggest that the films can be used for thermal control coatings inside buildings. In the poultry industry, films with high transmittance in the infrared region are needed in order to provide a source of heat for warming young chicks. In our view,  $Fe_2O_3/Cu_2S$  core-shell thin films,

deposited in this work meet this requirement. Hence, the films may be coated on the walls and roofs of poultry houses to admit infrared radiation (thermal portion of electromagnetic spectrum) into the building for warming purposes. This has the potential to reduce the cost of energy consumption associated with the use of electric bulbs, stoves and lamps as well the potential hazards associated with them. These findings are in tandem with the report of other authors in the literature [10, 22-24].

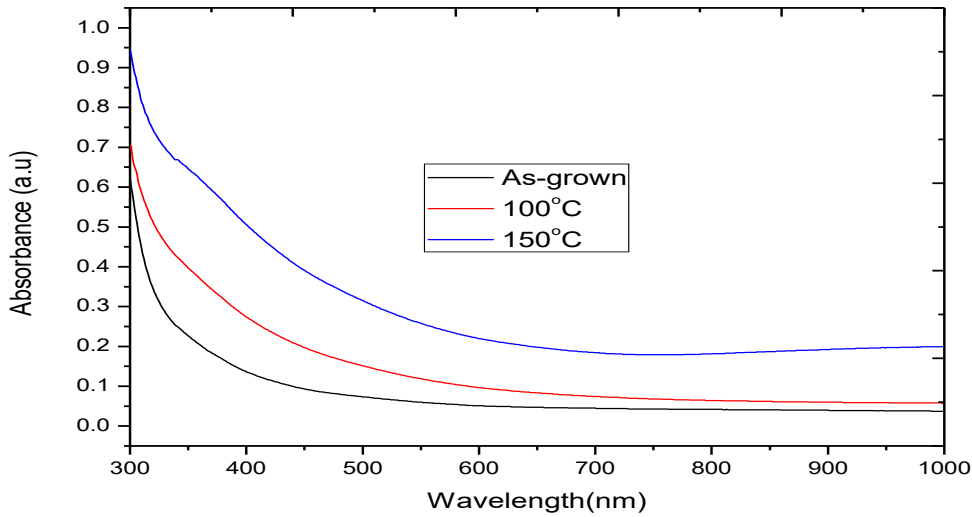


Fig.5: Absorbance against wavelength for  $Fe_2O_3/Cu_2S$  thin films at various annealing temperature

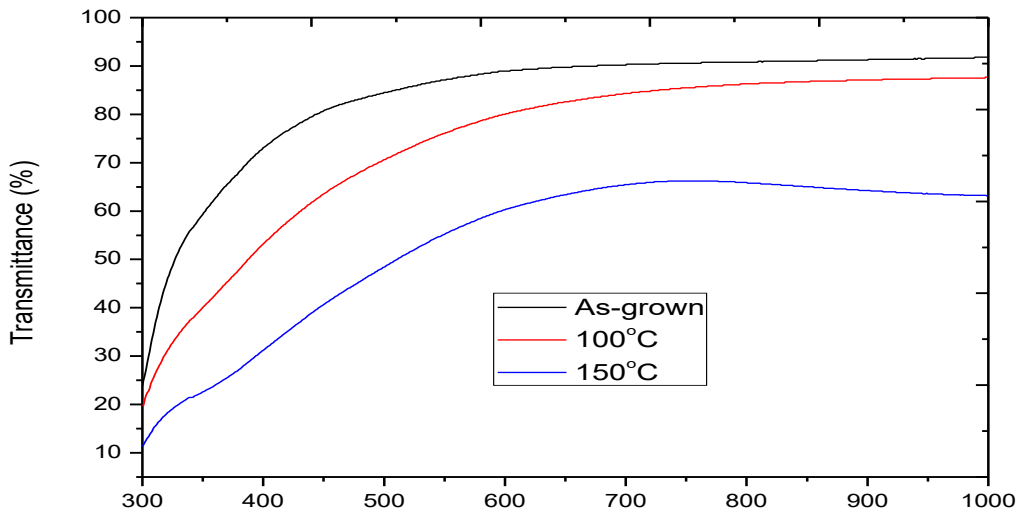


Fig.6: Transmittance against wavelength for  $Fe_2O_3/Cu_2S$  thin films at various annealing temperature

Fig.7 depicts the plot of absorption coefficient versus photon energy at various annealing temperature. The absorption coefficient ( $\alpha$ ) values of the films generally increased with photon energy (decreasing wavelength) exhibiting a maximum for the annealed layers. For as-grown film sample,  $\alpha$  increased from  $0.1 \times 10^6 \text{ m}^{-1}$  to  $1.45 \times 10^6 \text{ m}^{-1}$ . For annealed at  $150^\circ\text{C}$ ,  $\alpha$  increased from  $0.12 \times 10^6 \text{ m}^{-1}$  to  $1.63 \times 10^6 \text{ m}^{-1}$  while for annealed at  $200^\circ\text{C}$ ,  $\alpha$

increased from  $0.4 \times 10^6 \text{ m}^{-1}$  to  $2.20 \times 10^6 \text{ m}^{-1}$ . For materials with a direct band gap, the correlation coefficient of absorption of the photon frequency satisfies the equation [25].

$$(\alpha h\nu)^2 = A(h\nu - E_g) \tag{1}$$

where  $\alpha$ ,  $h$ ,  $\nu$  are absorption coefficient, planck's constant and photon frequency respectively.  $A$  is a constant and  $E_g$  is the band gap. Accordingly, the plots of  $(\alpha h\nu)^2$  versus  $h\nu$  for  $\text{Fe}_2\text{O}_3/\text{Cu}_2\text{S}$  thin films at various annealing temperature is shown in Fig.8.

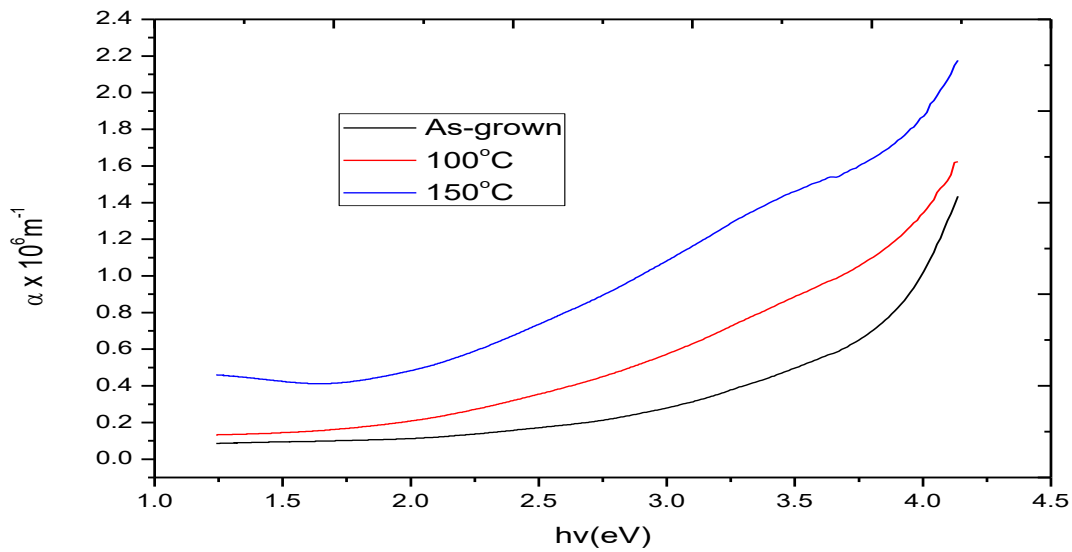


Fig.7: Plot of  $\alpha$  versus  $h\nu$  for  $\text{Fe}_2\text{O}_3/\text{Cu}_2\text{S}$  thin films at different annealing temperature

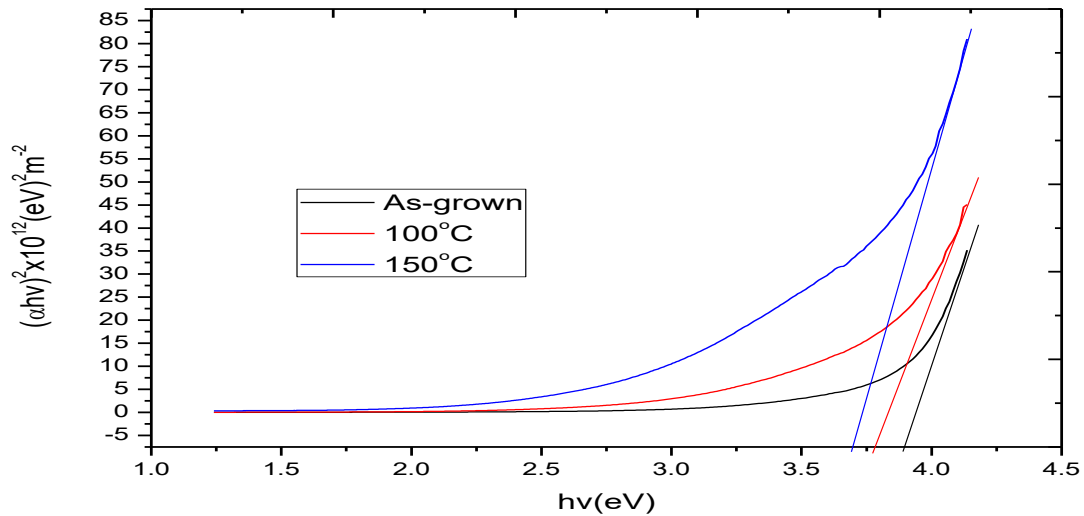


Fig.8. Plot of  $(\alpha h\nu)^2$  versus  $h\nu$  for  $\text{Fe}_2\text{O}_3/\text{Cu}_2\text{S}$  films at various annealing temperatures

The band gap energy values are 3.90eV, 3.80eV and 3.70eV for as-grown, annealed at 150°C and 200°C respectively. The value of the energy bandgap of the un-annealed layer was higher, compared to the annealed layers i.e, a clear indication of bandgap narrowing induced by the post deposition heat treatments. It is believed that thin film whose band gap values decrease with annealing temperature has particle distribution which increases with thermal annealing. The decrease in the energy bandgap of the heat treated layers was attributed to the increase in grain size and/or related phenomena, caused by the annealing effects [26]. These findings are in agreement with the report in the following references in the literature [9-13]. This is corroborated by the fact that the band gap can be expressed in terms of the effective mass approximation [27].

$$\Delta E_g = \frac{\frac{\hbar^2 \pi^2}{2R^2} \left( \frac{1}{M_e} + \frac{1}{M_h} \right) - (1.786e^2)}{\epsilon R} \quad (2)$$

Where  $M_e$  and  $M_h$  are the effective masses of the electrons in the conduction band and holes in the valance band respectively,  $\epsilon$  is the static dielectric constant of the material and  $\Delta E_g$  is the change in band gap of the semiconductor materials. The first term in the above equation represents the particle in-a-box quantum localization energy and has simple  $1/R^2$  dependence, where  $R$  is the particle radius. The second term represents the Coloumb energy with  $1/R$  dependence. Therefore, as  $R$  increases due to the increase in the crystallite size associated with high temperature annealing, the value of  $\Delta E_g$  will decrease. Processes like annealing which increases the particle size decreases the band gap and occurs in most cases with post deposition annealing [28]. Also as temperature increases, the band gap decreases because the crystal lattice expands and the interatomic bonds are weakened. Our findings are in agreement with the report of other authors [29, 30]. High value band gap semiconductors are used as window layer in fabrication of solar cell. The films of  $Fe_2O_3/Cu_2S$  deposited in this work have good absorption of visible spectrum of solar radiation and wide band gap energy. These properties make the films suitable as window layer for solar cell application. Fig.9 shows the plot of extinction coefficient versus photon energy.

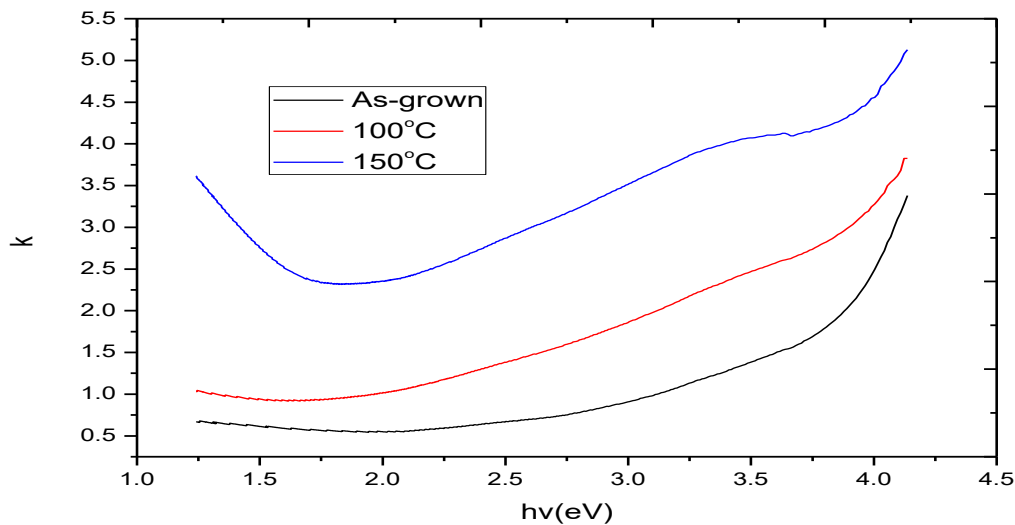


Fig.9. Plot of extinction coefficient versus  $h\nu$  for  $Fe_2O_3/Cu_2S$  films at various annealing temperatures

The extinction coefficient values are higher for the heated layers compared to the un-annealed layer. The maximum extinction coefficient values are 3.0, 3.5 and 5.0 for as-grown, annealed at 150°C and 200°C respectively. The refractive index ( $n$ ) of the thin films was calculated by the following relation [31].

$$n = \frac{1+R}{1-R} + \sqrt{\frac{4R}{(1+R^2)} - k^2} \quad (3)$$

where R is the normal reflectance and k is the extinction coefficient. As seen from Fig.10, the refractive index fluctuates between minima and maxima. It exhibited a downward trend within 3.90-4.15eV for as-grown sample, 3.75-4.20eV for annealed at 150°C and 2.75-4.05eV for annealed at 200°C.

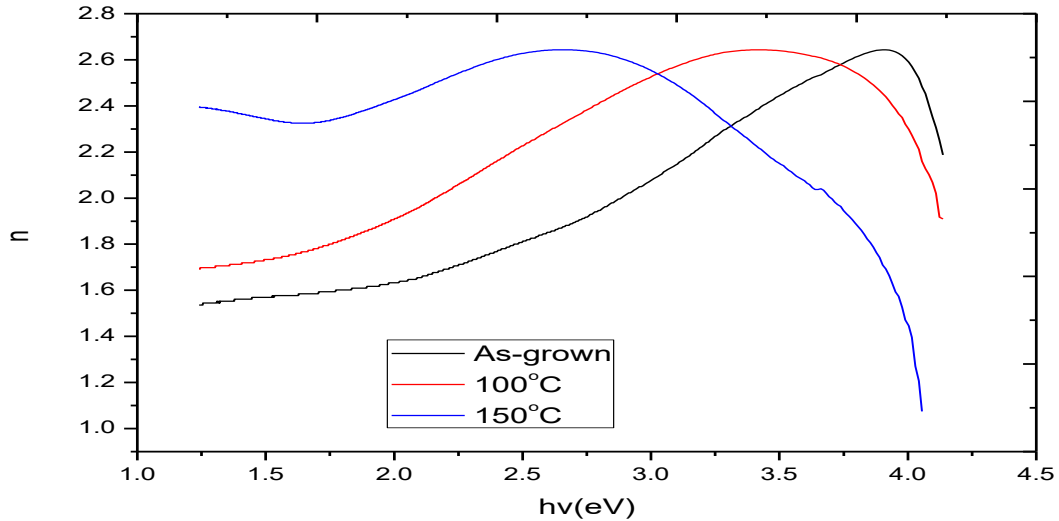


Fig.10. Plot of refractive index versus hv for Fe<sub>2</sub>O<sub>3</sub>/Cu<sub>2</sub>S films at various annealing temperatures

The complex dielectric constant is a fundamental intrinsic property of the material. The real part of the dielectric constant shows how much the speed of light slows down in the material, whereas the imaginary part shows how a dielectric material absorbs energy from an electric field due to dipole motion [32]. The knowledge of the real and the imaginary parts of dielectric constant provides information about the loss factor which is the ratio of the imaginary part to the real part of the dielectric constant [32]. The dielectric constant is a complex quantity that is related to the complex refractive index by the equation [33, 34].

$$\epsilon = \epsilon_r + \epsilon_i = (n - ik)^2 \quad (4)$$

Where  $\epsilon_r$  and  $\epsilon_i$  are the real and imaginary parts respectively of dielectric and  $(n - ik)$  is the complex refractive index. Hence,

$$\epsilon_r = n^2 - k^2 \quad (5)$$

$$\epsilon_i = 2ink \quad (6)$$

Figures 11 and 12 are plots of real and imaginary parts of dielectric constant versus photon energy respectively. A glance at fig.11, shows that the real dielectric curve is similar to that of the refractive index. This may be due to the mathematical relations used in computing the values of the two parameters. The range of values of the real dielectric constant are in agreement with the report of other authors [10, 11, 14, 21]. The imaginary dielectric constant generally increased with photon energy exhibiting a maximum for the heated layers.



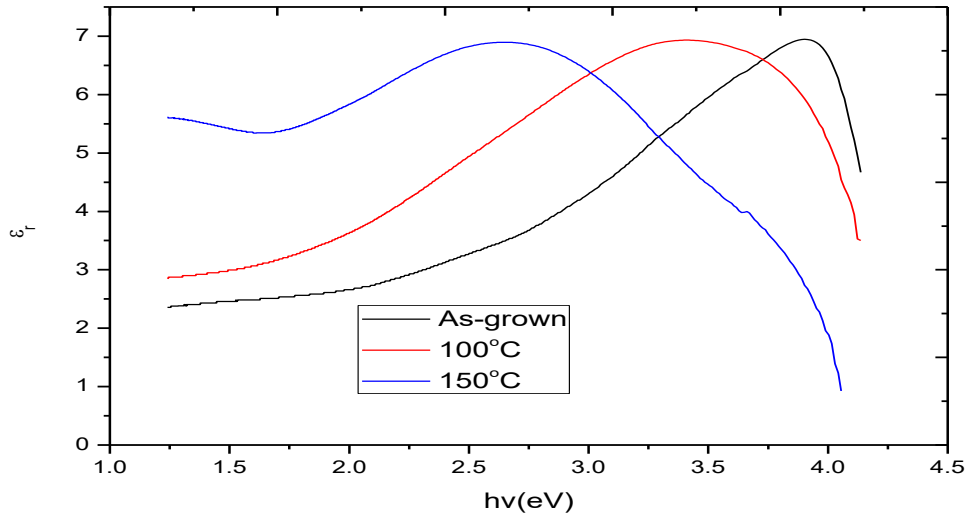


Fig.11. Plot of  $\epsilon_r$  versus  $h\nu$  for Fe<sub>2</sub>O<sub>3</sub>/Cu<sub>2</sub>S films at various annealing temperatures

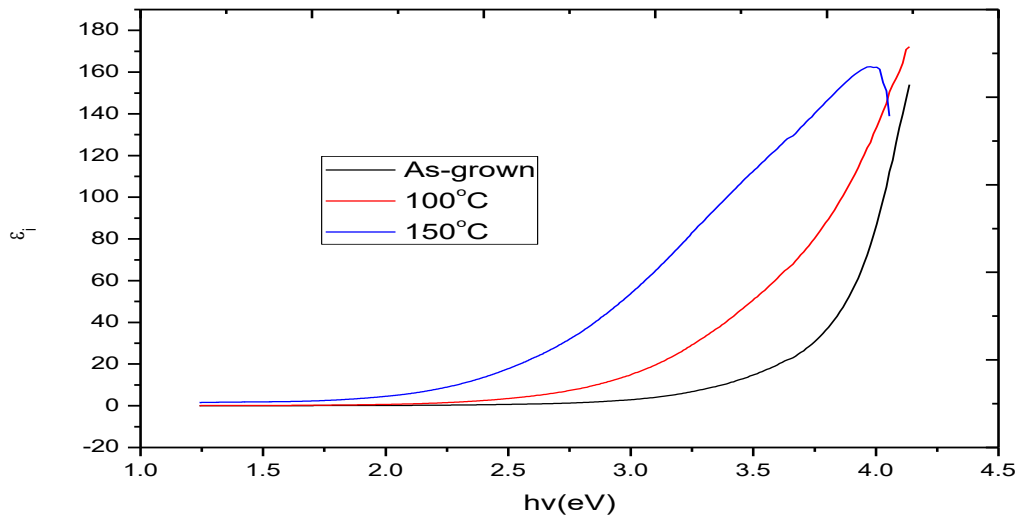


Fig.12. Plot of  $\epsilon_i$  versus  $h\nu$  for Fe<sub>2</sub>O<sub>3</sub>/Cu<sub>2</sub>S films at various annealing temperatures

#### IV. CONCLUSION

In this study, we have grown Fe<sub>2</sub>O<sub>3</sub>/Cu<sub>2</sub>S core-shell thin films on glass substrate by chemical bath deposition method. The deposited films were subjected to different annealing temperatures within the range 150-200°C. The microstructural, optical and solid state properties of the films were investigated. It was observed that all the optical parameters varied considerably with parameters of growth. The transmittance and band gap energy decreased with annealing temperature. The red shifting of the energy band gap with annealing temperature is a consequence of the

increase in particle size associated with increase in temperature. The high transmittance in the visible region and wide energy band gap is an indication that the films can be used as window materials in a heterojunction solar cell.

## REFERENCES

1. A.L. Fahrenbruch and R.H. Bube, "Fundamentals of solar cells" Academic Press New York, USA, 1983.
2. D. Su, H. S. Kim, W. S. Kim and G. Wang, "Synthesis of Tunable Porous Hematite ( $\alpha$ -Fe<sub>2</sub>O<sub>3</sub>) for Gas Sensing and Lithium Storage in Lithium Ion Batteries," *Microporous and Mesoporous Materials*, 149, 2012, 36-45.
3. S.L. Mammah, F.E. Opara, F.B. Sigalo, S.C. Ezugwu and F.I. Ezema, Annealing effect on the solid state and optical properties of  $\alpha$ -Fe<sub>2</sub>O<sub>3</sub> thin films deposited using the Aqueous Chemical Growth (ACG) methods, 3, 2012, 793-801.
4. B. Avijit, "Pickard's Manual of Operative Dentistry," Oxford University Press Inc., New York, 89, 2011.
5. A.S. Teja, P. Y. Koh, "Synthesis, Properties, and Applications of Magnetic Iron Oxide Nanoparticles," *Progress in Crystal Growth and Characterization Materials*, 55, 2009, 22-45.
6. T. Marin, C. Nada, P. Matjaz, S. Zoran, M. S. Dragana and S. Vojstav, "Synthesis, Morphology, Microstructure and Magnetic Properties of Hematite Submicron Particles," *Journal of Alloys and Compounds*, 509, 2011, 7639-7644.
7. J. Singh, M. Srivastava, J. Dutta and P. K. Dutta, "Preparation & Properties of Hybrid Monodispersed Magnetic Fe<sub>2</sub>O<sub>3</sub> Based Chitosan Nanocomposite Film for Industrial & Biomedical Application," *International Journal of Biological Macromolecules*, 48, 2011, 170-176.
8. C. Augustine, M.N. Nnabuchi, Band gap determination of chemically deposited lead sulphide based heterojunction thin films, *Journal of Non-Oxide Glasses*, 9(3), 2017, 85-98.
9. C. Augustine, M. N. Nnabuchi, F.N.C. Anyaegbunam, A.N. Nwachukwu, Study of the effects of thermal annealing on some selected properties of Heterojunction PbS-NiO core-shell thin film, *Digest Journal of Nanomaterials and Biostructures*, 12 (2), 2017, 523-531.
10. C. Augustine, M.N. Nnabuchi, Optical and solid state properties of chemically deposited CuO/PbS double layer thin film, *Materials Research Express*, 5(2), 2018, 1-11.
11. M.N. Nnabuchi, C. Augustine, Mn<sub>3</sub>O<sub>4</sub>/PbS thin film: Preparation and effect of annealing temperature on some selected properties, *Materials Research Express*, 5(3), 2018, 1-11.
12. C. Augustine, M.N. Nnabuchi, Band gap Determination of Novel PbS-NiO-CdO Heterojunction thin film for possible Solar Energy Applications, *Journal of Ovonic Research*, 13 (4), 2017, 233-240.
13. C. Augustine, M.N. Nnabuchi, F.N.C Anyaegbunam, C.U. Uwa, Annealing treatments and characterization of PbS-CdO core-shell thin film for solar energy applications, *Chalcogenide Letters*, 14 (8), 2017, 321-329.
14. C. Augustine, M. N. Nnabuchi, P. E. Agbo, F. N. C. Anyaegbunam, R. A. Chikwenze, C. N. Nwosu, P. N. Kalu, U. Uba, R. O. Okoro, S. O. Onyishi, Investigation of the effect of Lead ion (Pb<sup>2+</sup>) concentration on the optical and solid state properties of chemically deposited Mn<sub>3</sub>O<sub>4</sub>/Pb<sub>1-x</sub>S heterojunction thin films, *Journal of Ovonic Research*, 14, 2018, 339-350.
15. P.E. Agbo, M.N. Nnabuchi, and D.U. Onah, TiO<sub>2</sub>/Fe<sub>2</sub>O<sub>3</sub> Core-shell Thin Film for Application, *Journal of Ovonic Research*, 7(2), 2011, 29-35.
16. C. Augustine and M.N. Nnabuchi, Band gap determination of novel PbS-NiO-CdO heterojunction thin film for possible solar energy applications, *Journal of Ovonic Research*, 13(4), 2017, 233-240.
17. V. S. Reddy, K. Das, A. Dhar, S. K. Ray, "The effect of substrate temperature on the properties of ITO thin films for OLED applications," *Semiconductor Science and Technology*, 21, 2006, 1747-1752.
18. R.O. Okoro, M.N. Nnabuchi and C. Augustine, Post deposition temperature-dependent optical and solid state properties of chemically deposited ZnS/Fe<sub>2</sub>O<sub>3</sub> core-shell thin films, *Global Journal of Engineering Science and Researches*, 2018.
19. S.C. Ezeugwu, F.I. Ezeama, and P.U. Asogwa, *Chalcogenide Letters*, 7(5), 2010, 369-376.
20. P. E. Agbo, M. N. Nnabuchi, Core-Shell TiO<sub>2</sub>/ZnO Thin Film: Preparation, Characterization and effect of temperature on some selected properties, *Chalcogenide Letters*, 8 (4), 2011, 273-278.
21. P.N. Kalu, D.U. Onah, P.E. Agbo, C. Augustine, R.A. Chikwenze, F.N.C. Anyaegbunam and C.O. Dike, the influence of deposition time and annealing temperature on the optical properties of chemically deposited cerium oxide thin films, *Journal of Ovonic Research*, 14, 2018, 293-305.

22. A.E. Igweoko, C. Augustine, N.E. Idenyi, B.A. Okorie and F.N.C. Anyaegbunam, *Influence of processing conditions on the optical properties of chemically deposited zinc sulphide thin film*, *Materials Research Express*, 5, 2018, 036413.
23. R.A. Chikwenze, M.N. Nnabuchi, *Properties of lead selenide films deposited by chemical bath method*, *Chalcogenide Letters*, 7, 2010, 401-408.
24. Z. Jing, T. Xia, P. Yuan, F. Xiao, J. Zeng, *Core/ Shell Structured Zn/SiO<sub>2</sub> Nanoparticles: Preparation Characterization and Photo catalytic property*, *Applied Surface Science*, 257, 2010, 393-397.
25. Nwofe, P. A. and Agbo, P. E. (2017). *Annealing Treatments and Characterization of Nickel-Doped Antimony sulphide thin films*, *Journal of Non-Oxide Glasses*, 9 (1), 2017, 9-17.
26. Z. Jing, T. Xia, P. Yuan, F. Xiao, J. Zeng, *Core/ Shell Structured Zn/SiO<sub>2</sub> Nanoparticles: Preparation Characterization and Photo catalytic property*, *Applied Surface Science*, 257, 2010, 393-397.
27. J.D. Dipalae, S. Shaeed, S. Farha, G. Rrindam, B. Ravikiran, G. Anil, S. Ramphai, *Effect of Annealing on the Structural and Optoelectronic properties of CdS Thin Film*, *Advance in Applied Science Research*, 2 (4), 2011, 471-425.
28. M.M. Ali, *Characterization of ZnO thin films grown by chemical bath deposition*, *Journal of Basrah Researches (Sciences)*, 37 (3A), 2011, 49-55.
29. S. Sanjeev, D. Kekuda, *Effect of annealing temperature on the structural and optical properties of zinc oxide (ZnO) thin films prepared by spin coating process*, *IOP Conferences Series: Materials Science and Engineering*, 73, 2015, 012149.
30. J.S. Cruz, D.S. Cruz, M.C. Arenas-Arrocena, F.D.M. Flores, S.A.M. Hernandez, *Green synthesis of ZnS thin films by chemical bath deposition*, *Chalcogenide Letters*, 12 (5), 2015, 277-285.
31. R.A. Chikwenze, *Solution growth and characterization of binary selenide thin films for device applications*, *Ph.D Thesis, Department of Industrial Physics, Ebonyi State University, Abakaliki, Ebonyi State, Nigeria, 2012, 1-373.*
32. F. Wooten, *Optical properties of solids*, New York, Academic Press, 1972.
33. B.G. Mahrov, A. Hgfeldt, L. Dloczuk, and T. Dittrich, *Photovoltage study of charge injection from dye Molecules into transparent hole and electron conductors*, *Applied Physics. Letter*, 84(26), 2004, 5455-5457.